Can. J. Remote Sensing, Vol. 30, No. 5, pp. 827–839, 2004

Soil moisture estimation using an artificial neural network: a feasibility study

Hongli Jiang and William R. Cotton

Abstract. An artificial neural network (ANN) based algorithm is implemented and tested for soil moisture estimation. The ANN model is calibrated (trained) and validated (tested) with data including National Centers for Environmental Protection (NCEP) daily precipitation; normalized difference vegetation index (NDVI) data processed by the US Geological Survey Earth Resources Observations Systems (USGS EROS) data center; Geostationary Operational Environmental Satellite (GOES) based, cloud-masked infrared (IR) skin temperature produced by the University of Maryland; and soil moisture profiles measured over the Oklahoma (OK) Mesonet. The performance of the ANN model is evaluated by direct comparison between the soil moisture estimated by the ANN model and the Mesonet measurements and by examining the correlation between them. Strong correlation is demonstrated between the ANN estimates and Mesonet measurements for spatially averaged data. This work suggests that the ANN model is a promising alternative to soil moisture estimation. The advantage of the ANN approach to soil moisture estimation is that it can provide estimates having resolution commensurate with remotely sensed IR data and has the potential for worldwide coverage.

Résumé. On élabore et teste un algorithme basé sur les réseaux de neurones artificiels (RNA) pour l'estimation de l'humidité du sol. Le modèle RNA est étalonné (entraîné) et validé (testé) avec des données comprenant les précipitations quotidiennes NCEP, les données d'indice NDVI (« normalized difference vegetation index ») traitées par le Centre de données EROS de la USGS, les données IR de température de la peau masquées pour les nuages produites par l'Université du Maryland à partir des données GOES et les profils d'humidité du sol mesurés au-dessus du site Mesonet de l'Oklahoma (OK). La performance du modèle RNA est évaluée par comparaison directe entre l'humidité du sol estimée par le modèle RNA et les mesures du Mesonet, et en examinant la corrélation entre ces données. Il existe une forte corrélation entre les estimations RNA et les mesures Mesonet dans le cas des données spatialement moyennées. Ce travail suggère que le modèle RNA constitue une alternative prometteuse pour l'estimation de l'humidité du sol. L'avantage de l'approche RNA pour l'estimation de l'humidité du sol réside dans le fait qu'elle donne des estimations avec une résolution compatible avec les données IR de télédétection de même que dans la possibilité de couverture à l'échelle du monde qu'elle offre.
[Traduit par la Rédaction]

Introduction

Accurate estimation of soil moisture is essential for the successful simulations of boundary-layer evolution (e.g., Golaz et al., 2001), mesoscale circulations (e.g., Fast and McCorkle, 1991), and convection (e.g., Clark and Arritt, 1995; Gallus and Segal, 2000). However, in situ soil moisture observations are insufficient for direct real-time initialization. The limiting factors are the spatial and temporal distributions of those measurements. Many alternative methods and techniques are proposed and tested for retrieval of soil moisture. Among them are the direct use of passive microwave remotely sensed data (e.g., Vinnikov et al., 1999), assimilation of satellite-derived infrared (IR) heating rates into a numerical model (Wetzel et al., 1984; McNider et al., 1994; Jones et al., 1998a; 1998b), and combining satellite-derived values of IR skin temperature and vegetation index (Gillies and Carlson, 1995).

The low-resolution, passive microwave data are not very useful for cloud-scale and meso-scale applications because of the large footprint (from 25 km at 37 GHz to 150 km at 6.6 GHz). Data from these satellites are not ideal for measuring soil moisture in situations where there is significant vegetation cover (Owe et al., 1999). The National Oceanic and Atmospheric Administration (NOAA) advanced very high resolution radiometer (AVHRR) and geostationary operational environmental satellite (GOES) visible-infrared spin scan radiometer (VISSR) provide extensive spatial and temporal coverage. In addition, AVHRR data can be used to retrieve various geophysical parameters such as IR skin temperature (Price, 1984) and normalized vegetation index (Tucker, 1979) closely related to soil moisture. The recent launch of the advanced microwave scanning radiometer (AMSR) earth observing system (EOS) (AMSR-E) provides land products, including surface soil moisture with vegetation water content, surface temperature, and others, at a resolution as high as 5.4 km. Once these data become available, they can be used in various simulations that are highly sensitive to initial soil moisture distributions.

The purpose of this study is to test a new methodology capable of estimating soil moisture from remotely sensed IR data with high spatial and temporal resolution and the potential for worldwide coverage. The new methodology is an artificial neural network (ANN) based technique adapted from the ANN

Received 30 November 2003. Accepted 1 April 2004.

H. Jiang[1] and W.R. Cotton. Atmospheric Science Department, Colorado State University, Fort Collins, CO 80523, USA.

[1]Corresponding author (e-mail: jiang@atmos.colostate.edu).

model developed for precipitation estimation based on IR satellite data (Hsu et al., 1995; 1997; 1999; Sorooshian et al., 2000).

Although soil water content can be related to meteorological, surface, and vegetation variables through the soil water and energy balance equations (e.g., the soil water, energy, and transpiration (SWEAT) model) (Daamen and Simmonds, 1996), the relationships among these variables are highly nonlinear. The methodology of ANN has been used in applications where the characteristics of the processes are difficult to describe using simple physical equations. A neural network learns the input–output relationship through a training process.

Our objective is to select the minimum number of remotely sensed variables that are highly correlated with soil moisture content as the input to the ANN model. Additional variables relating to soil and vegetation types will be incorporated into the input data later. Using three independent datasets including IR skin temperature, normalized difference vegetation index (NDVI), and National Centers for Environmental Protection (NCEP) daily precipitation as primary inputs to the ANN model, we examined the applicability and potentials of the ANN model in soil moisture estimation. The term soil moisture used throughout this study is defined as volumetric soil moisture (VSM in units of m^3_{water}/m^3_{soil}), an average over the root zone. The process of evaluating the performance of the ANN model consists of calibration (training) and validation (testing). During the calibration and validation, in situ observations of soil moisture from the Oklahoma (OK) Mesonet are used to adjust the ANN parameters in the direction of minimizing the differences between the ANN output and the observations. Although the Oklahoma meso-network covers only Oklahoma, it provides better spatial and temporal coverage (115 sites, data is taken at 15 min time interval) than most measurement networks, such as the Illinois State Water Survey and the Soil Climate Analysis Network (SCAN) of the US Department of Agriculture (USDA). The SCAN data have good temporal coverage (30 min interval) but an average of only one station per state, whereas the Illinois State Water Survey consists of 14 sites in Illinois.

In the following sections, we provide a brief summary of the ANN model, outline the strategy for selecting and testing input variables for the ANN model, present the statistical results from selected input variables, and compare the model results with antecedent precipitation index estimates.

Artificial neural networks

The ANN model used in this study was developed by a group of scientists at the University of Arizona. The ANN methodology has been successfully applied to wide-area rainfall estimation over several locations. The ANN uses a modified counter-propagation network model (CPN), which incorporates satellite imagery as the basis of areal rainfall estimates with available rain-gauge, radar, and other observations applied to an automated "training" or self-calibration process that significantly improves the satellite estimates. Readers are referred to Hsu et al. (1995; 1997; 1999) for a detailed description, evaluation, and discussion of the overall performance of the model. A brief summary is given here.

Many ANN structures have been proposed and tested since the 1950s. The most widely employed structures include multilayer, feed-forward neural networks (MFNNs), also known as the back-propagation algorithm (BPA) (Rumelhart et al., 1986); self-organizing feature maps (SOFM) (Kohonen, 1984); and counter-propagation networks (CPNs) (Hecht-Nielsen, 1988). The ability to learn is one of the most important characteristics of ANN models. Despite differences in detailed structures and the number of layers among ANN models, ANN models perform two basic functions: (*i*) a learning process that classifies inputs to hidden layers, and (*ii*) an optimization process that maps the classified inputs to outputs.

The CPN used in this study is a hybrid network that combines two basic networks, the SOFM and Grossberg linear networks (Hecht-Nielsen, 1988). The basic structure of the ANN has three layers: the input layer, the hidden layer, and the output layer. The three-layer structure consists of two functional components. The input–hidden component detects and classifies features and nonlinearity in the input data (x_i) and then maps them into clusters in the hidden layer (y_j) by using the SOFM learning algorithm. The SOFM is trained through an unsupervised learning using only the input data in the training process. The classified signal y_j is connected to input variables x_i through a weight parameter W_{ij}. Thus the process of training on SOFM consists of presenting input vectors one by one from the input dataset to the hidden layer of the network. **Figure 1** shows the schematic diagram of the ANN model.

Once the SOFM is trained, the input data are processed into a number of clusters, and then an optimization method is used in the second component to search for the weights (network parameters) that best match network outputs and targets. The linear mapping (LM) in the hidden–output component relates the classified inputs (y_j) to the output variables (z_k) through a weight parameter V_{jk}. The linear mapping algorithm compares and adjusts the ANN parameters using a negative gradient algorithm in which the mean square error between the ANN output and the target data (z_o) is minimized. The target data (z_o) are usually the observational data. Once the network error has decreased to less than a specified threshold value, the network has converged and is considered to be trained. The two components are trained separately. This feature is especially useful when dealing with a large amount of data.

Another useful feature of this ANN model is that it uses an adaptive procedure that recursively updates the network parameters when additional observational data are available. Ideally, one would use a dataset that contains seasonal and topographic changes to train the ANN model. Often the observational data of interest are unavailable. For situations lacking sufficient data, the model will be trained with a limited amount of observational data initially to obtain preliminary estimates of the network parameters. This process is considered

as model calibration. Subsequently, the network parameters are updated through sequential training when additional data from either different seasons or geographic locations become available. During the sequential training, small adjustments are made to the parameters and the model performance will be improved. The sequential training is treated as the model validation, testing, or simulation.

Selection of input variables

One of the critical issues in training the ANN model is to select input variables that are highly correlated with soil moisture. Previous studies have shown good correlation between soil water content and IR skin temperature and NDVI (Gillies and Carlson, 1995), and between IR heating rate and the antecedent precipitation index (API) (Wetzel and Woodward, 1987). After collecting these variables from independent datasets, we evaluated the correlation and dependency among these variables.

Data sources

Although satellite data are readily available, it is still very time consuming to process a large amount of satellite data. To focus our attention on understanding and evaluating the ANN model without spending a large effort dealing with data processing, we acquired four independent datasets: NCEP daily precipitation data; GOES-based, cloud-masked, IR skin temperature processed by the University of Maryland; NDVI data processed from AVHRR data by the US Geological Survey Earth Resources Observations Systems (USGS EROS) data center; and the OK Mesonet volumetric soil moisture (m^3_{water}/m^3_{soil}), then vertically averaged over four layers (5, 25, 60, and 75 cm).

The skin temperature data contain the hourly gridded data over the US (24–54°N, 65–126°W,) with a resolution of 0.5° × 0.5° latitude–longitude. The NDVI data are composited biweekly gridded data over the US (22.48–48.4°N, 75.41–128.52°W), with a resolution of 0.125° × 0.125° latitude–longitude. The NDVI data provide seasonal variations in the vegetation pattern. The NCEP daily precipitation data are collected from approximately 6000 gauge stations per day from the River Forecast Center (RFC) and several hundred gauge stations per day from the Climate Anomaly Data Base. They are gridded data covering the US (20–60°N, 60–140°W) with a resolution of 0.25° × 0.25° latitude–longitude.

Study area

All data are first projected and linearly interpolated onto an equally spaced grid with a resolution of 0.5° × 0.5° latitude–longitude. The OK Mesonet soil moisture station data are interpolated onto the same grid after applying the Barnes objective analysis scheme (Barnes, 1973). Because the OK Mesonet covers Oklahoma only, our study area is limited to Oklahoma (33.75–37.25°N, 95.25–100°W) excluding the panhandle.

Data quality

Quality assurance is performed by the Mesonet, and quality flags are provided in the data. Only data marked as good are used in this study. It should also be noted that the missing data for skin temperature are supplemented with output from the North American land data assimilation system (NLDAS). NLDAS is a very advanced land surface modeling system. Readers are referred to Mitchell et al. (2004), who provide an extensive overview of this multi-institutional and multipartner effort.

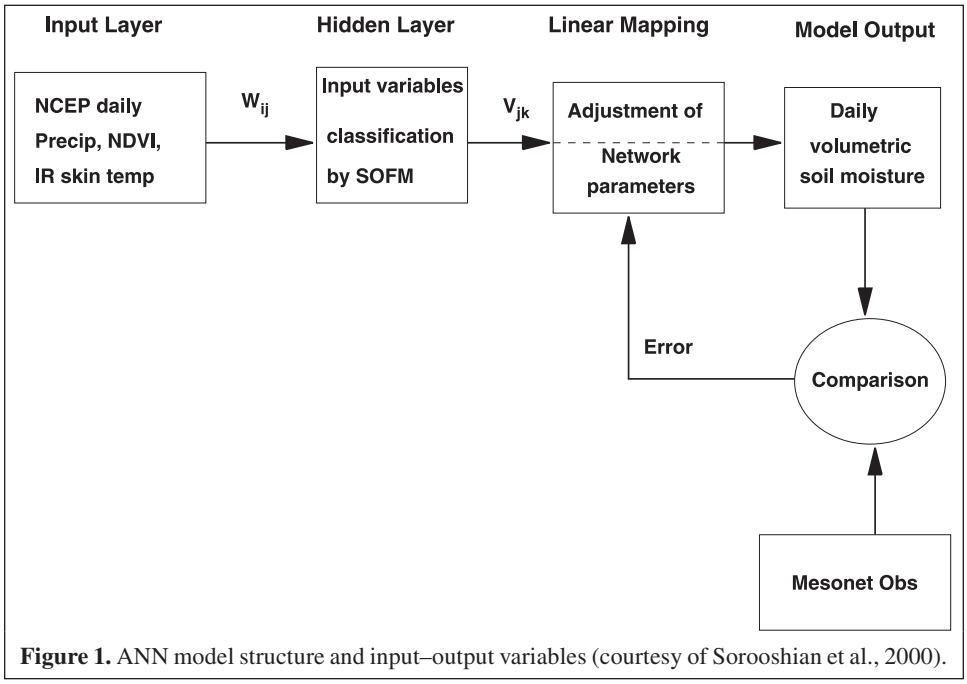

Figure 1. ANN model structure and input–output variables (courtesy of Sorooshian et al., 2000).

Data processing

Data from the warm months (May–September) in 1999 and 2000 are selected, and both the spatial and temporal datasets are used. They are organized as follows. First, all the data are in the equally spaced grid, with spatial resolution of 0.5° × 0.5° latitude–longitude and daily temporal resolution. Second, each input variable is written in the same storage order as a FORTRAN data array at the given time interval. For any given variable var1(NX × NY × NT), NX varies from west to east first, and NY varies from south to north second at time 1, and then both NX and NY repeat for time 2 until the final time, where NX and NY are the total number of data points in the east–west and north–south directions, respectively, and NT is the time (total number of days). Each input variable occupies a single column in the final data matrices.

Input variables

To select the input variables that are strongly correlated with the output, many numerical experiments were conducted with various input variables. Some of the variables tested include temperature difference $\Delta T = T_{skin} - T_{air}$, where T_{air} is the temperature measured at 2 m above the surface and T_{skin} is the effective radiative temperature at the surface and is converted from longwave radiation; T_{skin}/RAD_{net}, where RAD_{net} is the net surface radiative flux; and daily rain rate. These variables are not selected because of limitation in data availability, data quality, or low correlation with the root-zone volumetric soil moisture. The variables that produced the best correlations between the estimated and observed soil moisture are selected to train the ANN model. The ANN model is trained with the IR skin temperature (T_s), NDVI (N^*), and previous 30 day accumulated precipitation as the input variables. For simplicity, NDVI is normalized as follows:

$$N^* = (NDVI - NDVI_{min})/(NDVI_{max} - NDVI_{min}) \quad (1)$$

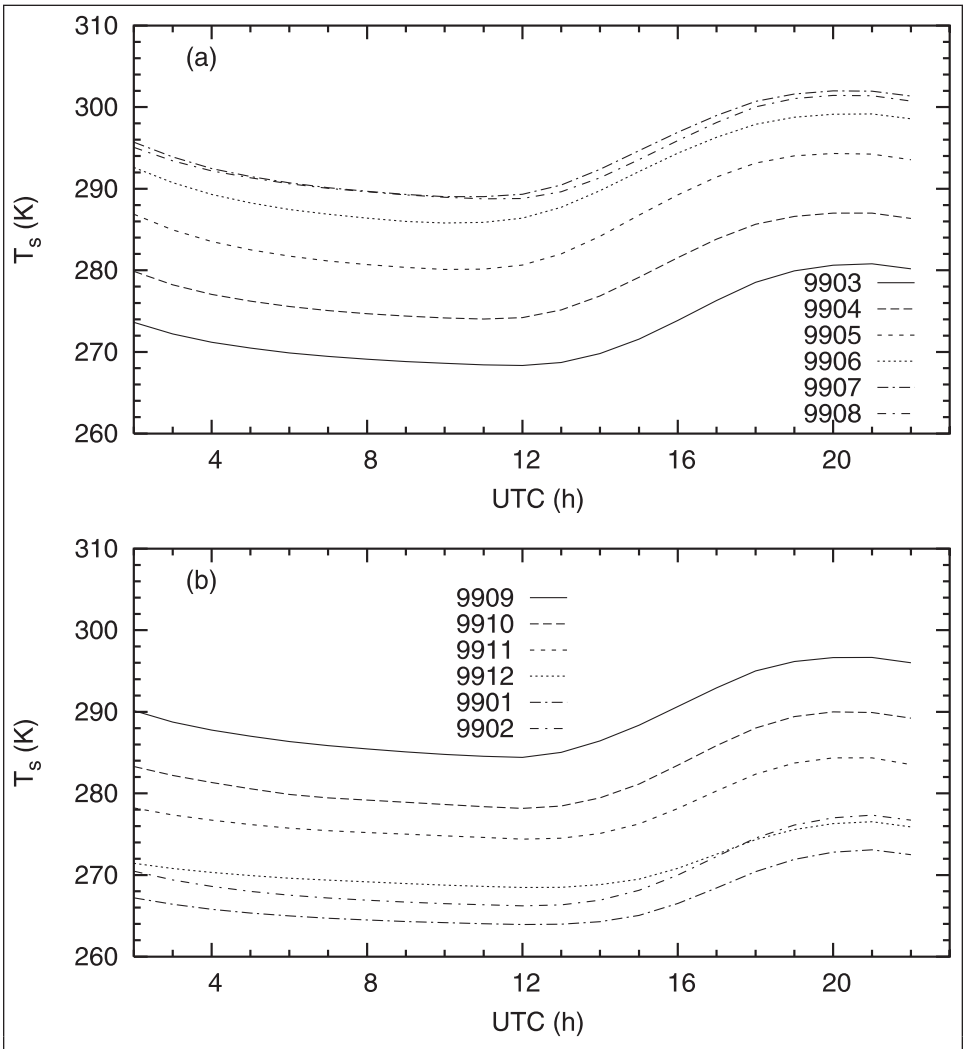

Figure 2. Spatially averaged skin temperature as a function of time for 1999: (a) March (9903) to August (9908); (b) January (9901), February (9902), and September (9909) to December (9912).

where N^* ranges from 0 to 1.

To understand how skin temperature and heating rate (defined as $dT_s/dt = T_s(t + 1) - T_s(t)$, where t is time) derived from skin temperature between the hourly data evolve owing to the incident solar heating during the course of the day, the spatially averaged skin temperatures and heating rate over the study domain for all of 1999 are plotted as a function of time in **Figures 2** and **3**.

The skin temperature (**Figure 2**) increases mainly from sunrise to the afternoon (12 UTC – 20 UTC) for all the months shown, and T_s becomes warmer continuously from January to August and colder from September thereafter. The rate of change of the skin temperature exhibits differences as the season progresses (**Figure 3**). The main feature is that it becomes positive between 10 UTC and 12 UTC and reaches a maximum in the midmorning but at a progressively slower rate from May to December, and then decreases back to zero almost at the same rate for all the data shown. For the cold months (**Figure 3b**), the duration while the rate of change of the skin temperature remains positive is much shorter and the maximum rate is smaller than that of the warm months. The fact that the major differences in the distribution of the heating rate versus time are present mainly in the earlier part of the day suggests that we only need to process data from early morning to noon when cloud-free views of the surface are more frequent (McNider et al., 1994) for daily soil moisture estimation.

After a similar averaging process is applied to the Mesonet stations data, the volumetric soil moisture does not display significant sensitivity in response to solar heating (not shown). Without averaging, the data are too noisy to show any meaningful relationship. Wetzel et al. (1984), however, showed in their study that variation in soil moisture among other variables is sensitive to the midmorning change in skin temperature.

Figure 4 shows the scatterplots of the variables of interest and the correlation coefficients and linear regression lines using

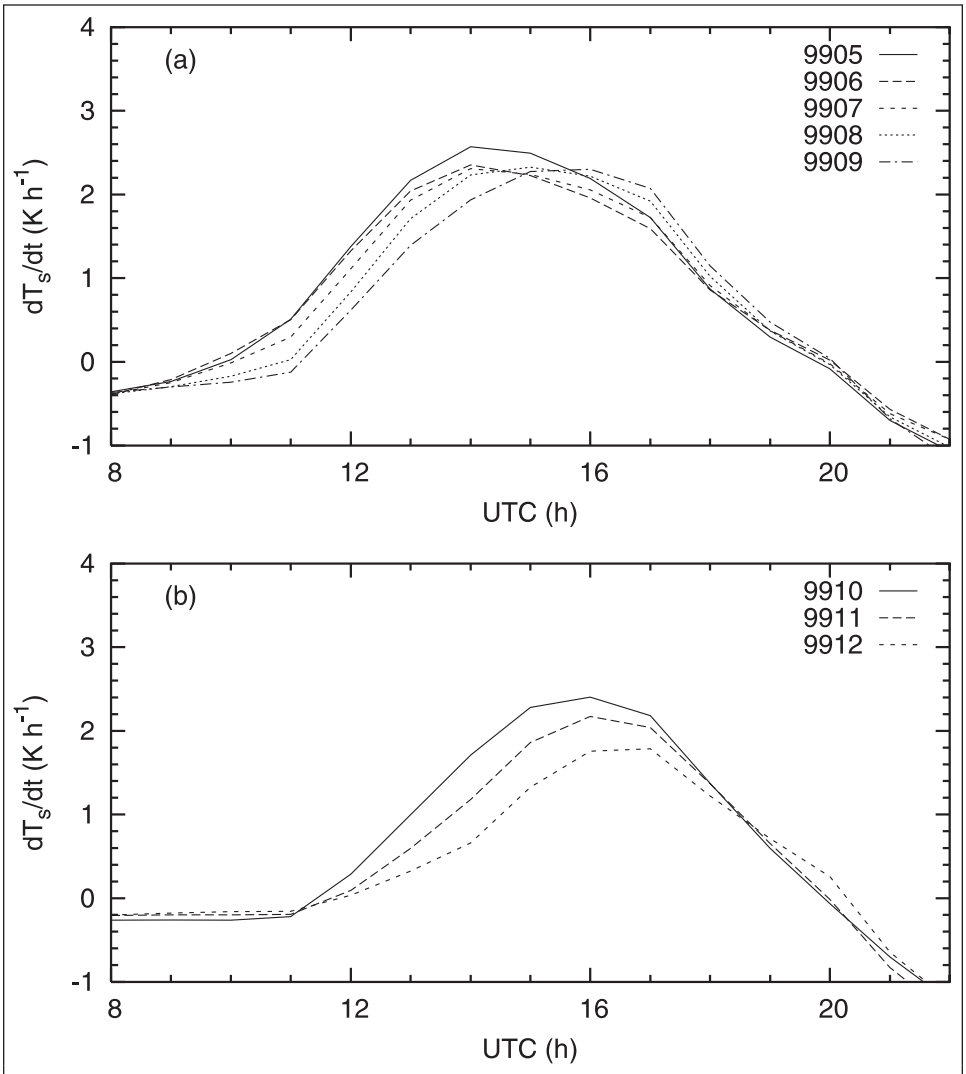

Figure 3. Spatially averaged rate of change of skin temperature (dT_s/dt) as a function of time (t) for 1999: (a) warm months, May (9905) to September (9909); (b) winter months, October (9910) to December (9912).

daily composites with data from the warm months of 1999. The soil moisture is vertically averaged over the four layers (0–75 cm) of Mesonet VSM and spatially averaged over all Mesonet stations. The NCEP data and the skin temperature are spatially averaged over the study domain. The skin temperature is negatively correlated with the VSM, with a correlation coefficient R equal to –0.416 (**Figure 4a**), suggesting that soil moisture decreases when solar insolation increases. The NDVI data are moderately correlated with VSM (R = 0.7771). The strongest correlation (R = 0.9343) is shown between daily averaged VSM and the previous 30 day accumulated NCEP precipitation.

The correlation coefficient between any two variables (v_1, v_2) is defined as

$$R = \sqrt{\frac{\mathrm{cov}(v_1, v_2)^2}{\mathrm{var}(v_1)\mathrm{var}(v_2)}} \tag{2}$$

where $\mathrm{cov}(v_1, v_2)$ is the covariance of v_1 and v_2, and $\mathrm{var}(v_1, v_2)$ is the variance of v_1 or v_2. R is in the range [–1, 1]. The closer the

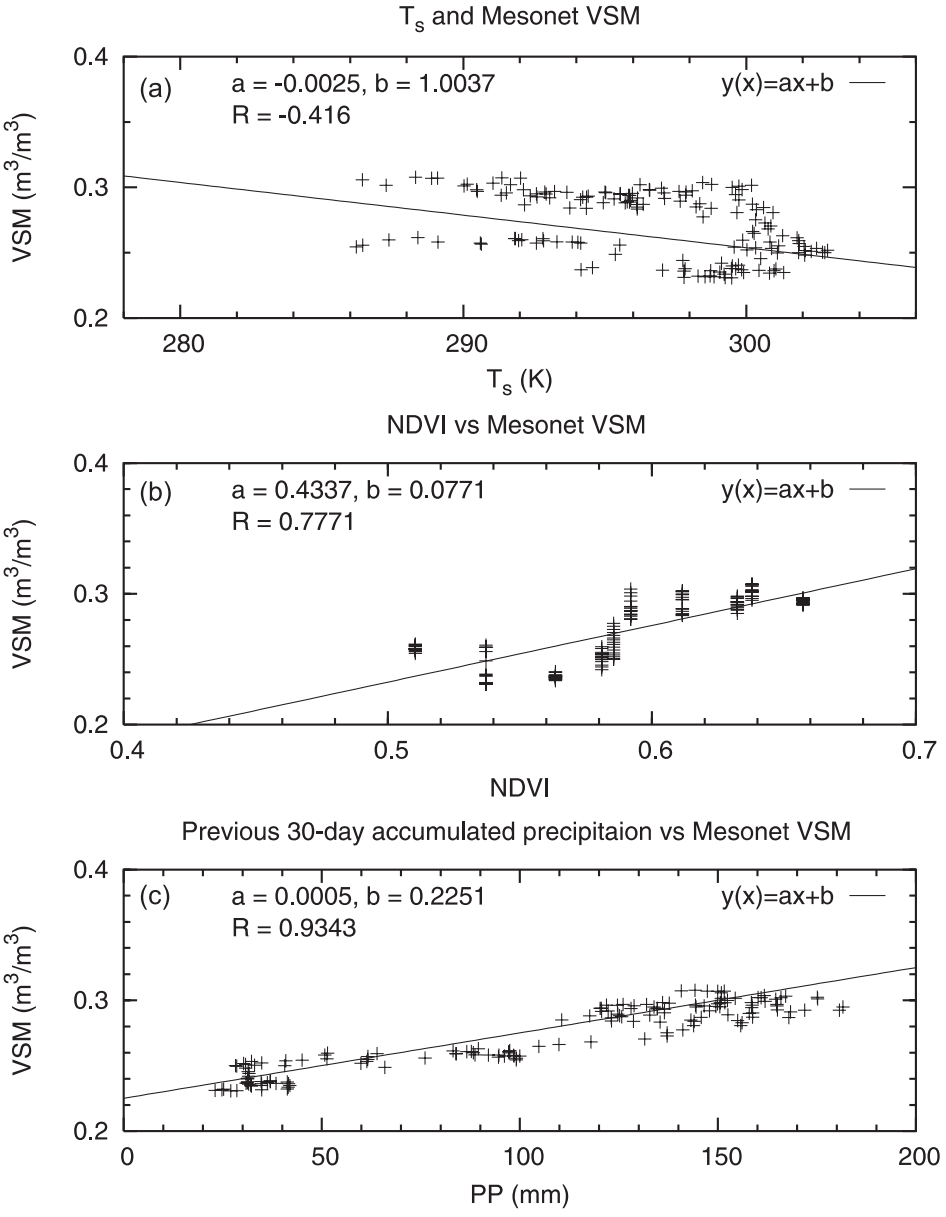

Figure 4. Scatterplots of correlation between the input variables and Mesonet-measured volumetric soil moisture (VSM) for the warm months in 1999: (a) skin temperature (in K) versus Mesonet VSM (in m^3_{water}/m^3_{soil}), where the Mesonet VSM is vertically averaged over four layers (0, 25, 60, and 75 cm); (b) NDVI versus Mesonet VSM; (c) previous 30-day accumulated precipitation versus Mesonet VSM. All data are spatially averaged over the study domain (Oklahoma), and the correlation coefficient (R) and linear regression fitting coefficients (a, b) are indicated for each relationship.

value is to 1 (–1), the more positively (negatively) correlated the two variables.

Evaluation of ANN training results

Three criteria are used to evaluate the performance of the ANN model, namely the correlation coefficient, root mean square error (RMSE), and bias (BIAS). The correlation coefficient is defined in Equation (2), and BIAS is defined as follows:

$$\mathrm{BIAS} = \frac{\sum_N (\mathrm{VSM_{ann}} - \mathrm{VSM_{meso}})}{N} \tag{3}$$

where $\mathrm{VSM_{meso}}$ is the OK Mesonet observed volumetric soil moisture, vertically averaged over the four layers (0–75 cm); $\mathrm{VSM_{ann}}$ is the similar quantity from the ANN estimate. If BIAS is greater (less) than zero, the ANN model overestimates (underestimates) the VSM. RMSE is defined as

$$\mathrm{RMSE} = \sqrt{\frac{\sum_N (\mathrm{VSM_{ann}} - \mathrm{VSM_{meso}})^2}{N-1}} \tag{4}$$

As the value of RMSE approaches zero, the model results closely match the observations. Data from the warm months (May to September) in 1999 are used to train the ANN model.

Figure 5a shows the VSM spatially averaged over all available OK Mesonet stations and the ANN model estimate as a function of time for 1999. The ANN model underestimates

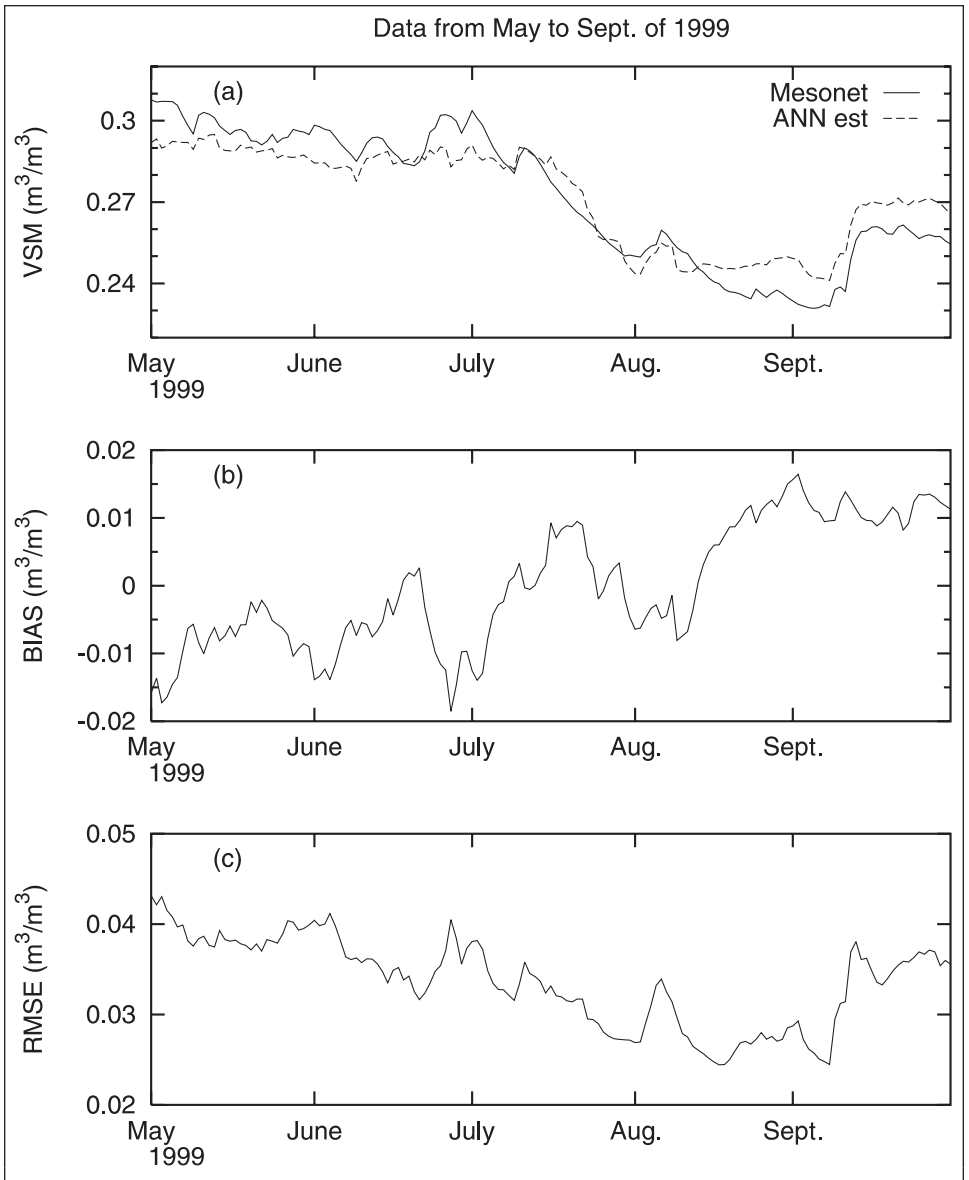

Figure 5. Statistical results of the ANN soil moisture estimation from training with data from the warm months (May–Sept.) of 1999: (a) spatially averaged VSM; (b) bias (BIAS); (c) root mean square error (RMSE).

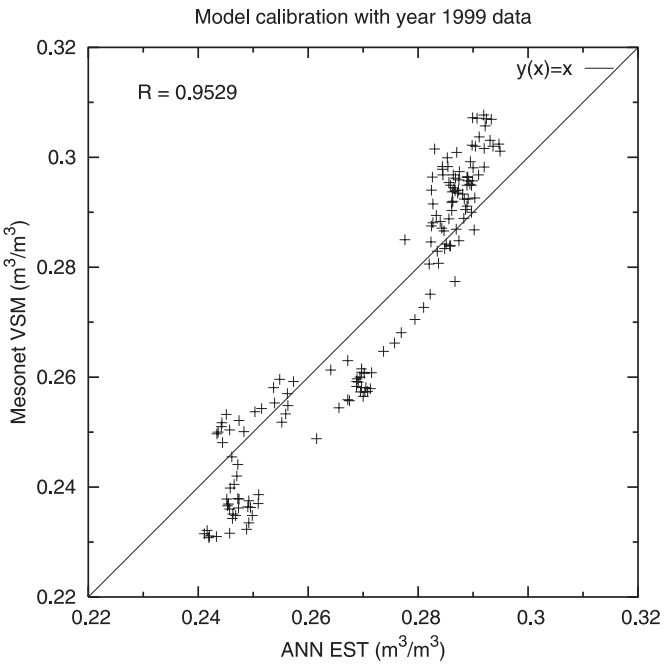

Figure 6. Scatterplot of estimated (ANN EST) and observed (Mesonet VSM) soil moisture for the same data as shown in **Figure 5**. The correlation coefficient *R* equals 0.9529, and the solid line represents points where the estimated soil moisture equals the observed soil moisture.

VSM from May to mid-July of 1999 (negative BIAS) and overestimates VSM from mid-July to the end of September of 1999 (**Figures 5a**, **5b**). The RMSE (**Figure 5c**) decreases slightly from May to September, indicating improvement in the performance of the ANN model.

Although the scatterplot of the spatially averaged VSM between the Mesonet data and the ANN estimate (**Figure 6**) shows strong correlation (R = 0.9529), it reveals that the ANN model tends to overestimate when VSM is low and underestimate when VSM is high, as seen in **Figures 5a** and **5b**.

Spatial distributions from training results for 1 July 1999 (**Figure 7**) are plotted along with the observations (Mesonet data) to determine where the model has missed. A detailed comparison of **Figures 7a** and **7b** reveals that the ANN model has missed most of the fine features.

Results after sequential training

The trained ANN model is tested with data from the warm months (May to September) of 2000 to see if it can produce soil moisture values close to the observations. The testing process only performs the second component shown in **Figure 1**, thus information stored in the SOFM hidden layer from the training data will be used during testing.

A plot similar to that of **Figure 5** is generated with the data from the warm months of 2000 (**Figure 8**). **Figure 8a** shows that the ANN estimate closely matches the Mesonet data. The bias (**Figure 8b**) has reduced to about a third of that shown in

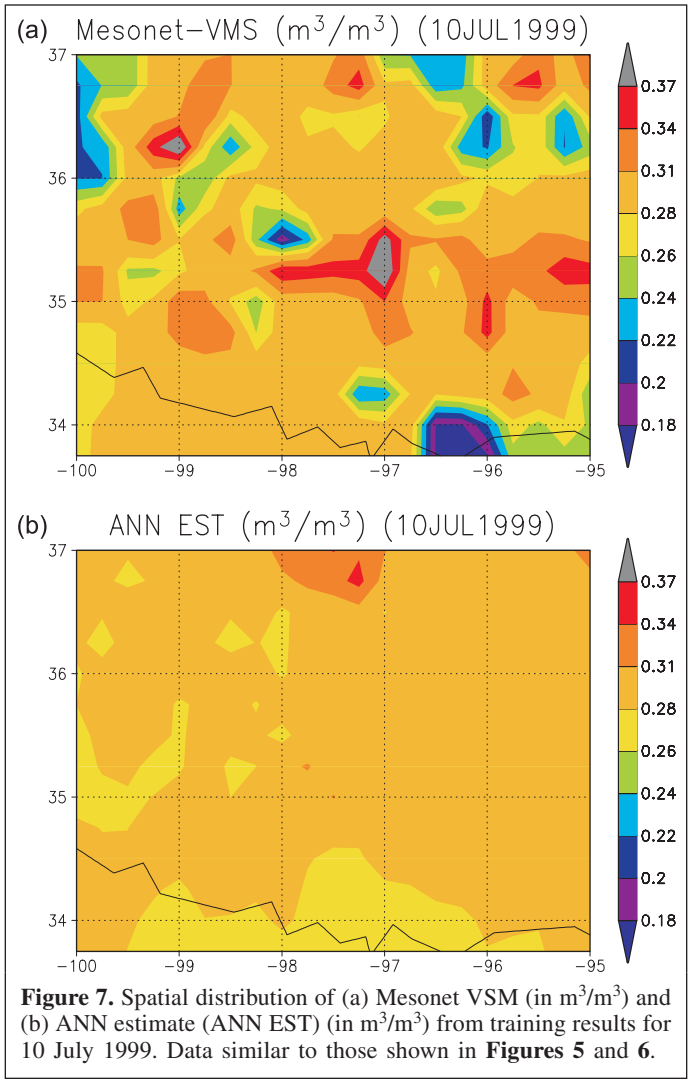

Figure 7. Spatial distribution of (a) Mesonet VSM (in m^3/m^3) and (b) ANN estimate (ANN EST) (in m^3/m^3) from training results for 10 July 1999. Data similar to those shown in **Figures 5** and **6**.

Figure 5b, and the RMSE (**Figure 8c**) is slightly higher than that shown in **Figure 5c**. It should be noted that the data shown are spatially averaged over the study domain. The averaging process has resulted in a reduction in the bias, but the higher RMSE in **Figure 8c** indicates a larger fluctuation than that shown in **Figure 5c**.

The scatterplot of the spatially averaged VSM between the Mesonet data and the ANN estimate (**Figure 9**) shows a stronger correlation (R = 0.9971), with a majority of the data points following the straight line that represents points where the estimated VSM is equal to that observed.

A plot similar to that of **Figure 7** is presented for 1 July 2000 along with the Mesonet data (**Figure 10**) to evaluate the ANN model performance after sequential training. A comparison of **Figures 10b** and **7b** reveals the improvement in the ANN model after sequential training. **Figure 10b** shows that the ANN model has captured some of the finer details, such as the wet spot near the east-central region in the plot.

It is clear that the ANN model does not produce a perfect match to the spatially distributed Mesonet data, largely owing to the limitation of available data. As discussed by Hsu et al.

(1997) when the ANN model was calibrated with a very limited amount of data, the model may not be able to recognize some of the patterns in the input data. Improvement can be achieved by sequential training with more extensive datasets, as shown in the comparison between **Figures 10b** and **7b**.

Both the training and testing data used to obtain the aforementioned results are for the warm months (May to September of 1999 and 2000, respectively). To examine whether the trained model is capable of producing the soil moisture close to the observations when applied to any geographical locations or seasons, the ANN model is tested with the data from October to December of 2000.

Table 1 shows a comparison of the correlation coefficients for the relationships between the input variables and spatially averaged Mesonet VSM for the two different datasets (one for warm months and one for winter months). The skin temperature is negatively correlated with VSM (row 1) in both cases. The correlation coefficients between the vegetation data (NDVI) and VSM (row 2) and between precipitation and VSM are much lower for the winter months (October–December). It is likely that the soils are moistened to field capacity during the winter months. Thus, without evapotranspiration, the water content of the soil will remain constant with varying precipitation.

Despite the differences in the input data (**Table 1**), the spatially averaged results produced by the ANN model match the Mesonet observation (**Figure 11a**) for the winter months as well. Compared with **Figure 8c**, however, the RMSE (**Figure 11c**) increases with time, suggesting that the performance of the ANN model deteriorates over time.

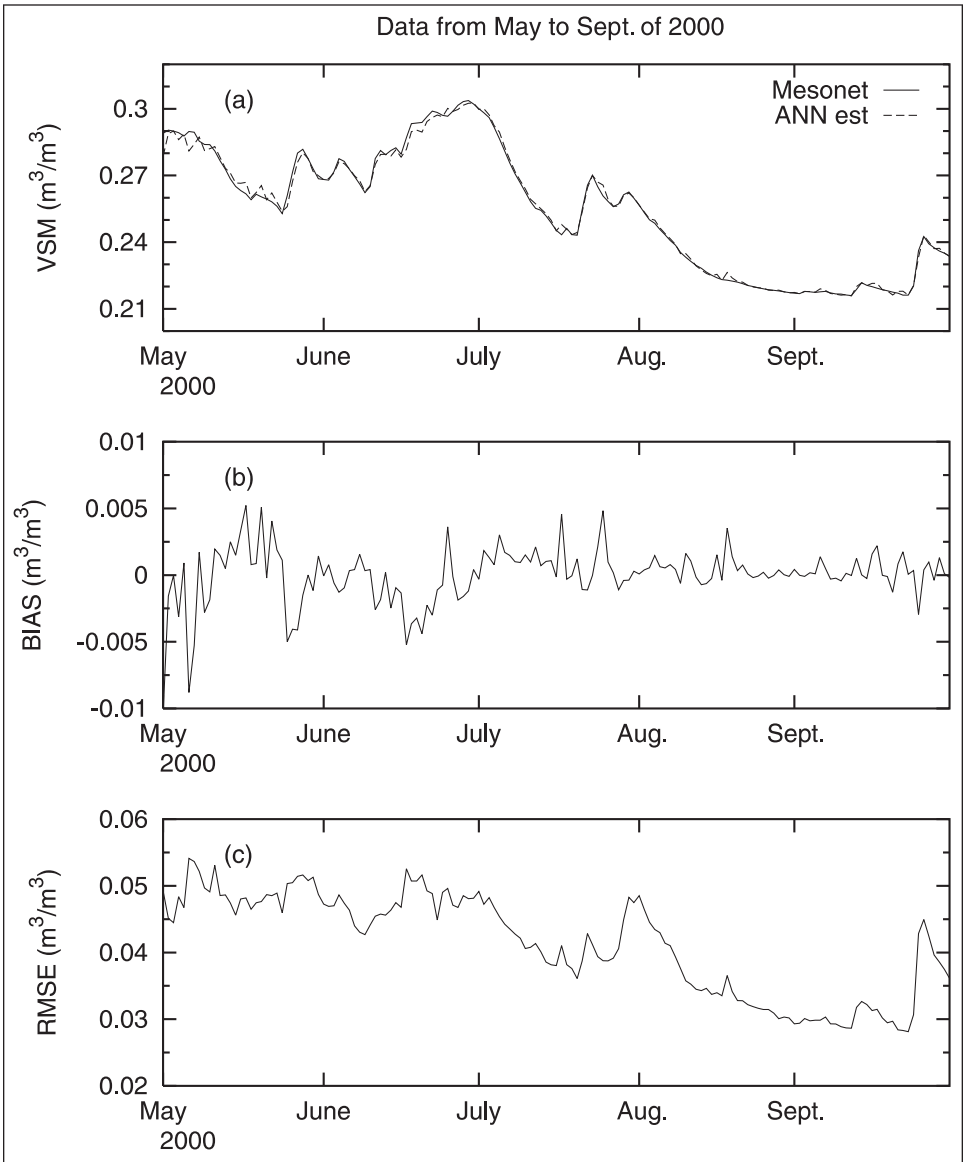

Figure 8. Similar to **Figure 5** except for comparison of statistical results from testing with data from the warm months of 2000 (May–Sept.).

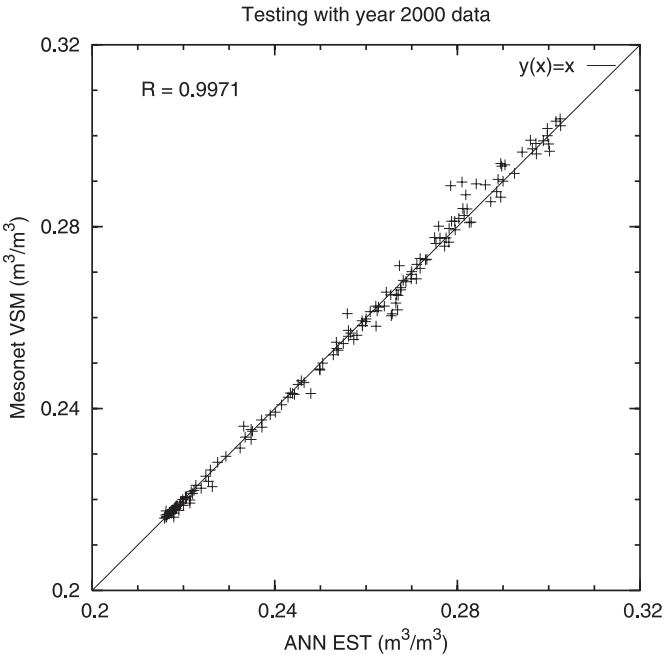

Figure 9. Similar to **Figure 6** except for testing with data from the warm months of 2000. The correlation coefficient R equals 0.9971, and the solid line represents points where the estimated soil moisture equals the observed soil moisture.

Comparison with antecedent precipitation index (API)

The antecedent precipitation index (API) has long been considered a good estimate of soil moisture amounts. Previous studies have shown good agreement between API estimates and observed soil moisture amounts (Blanchard et al., 1981; Choudhury and Blanchard, 1983; Wetzel and Woodward, 1987; Chang and Wetzel, 1991; Teng et al., 1993). API is given by

$$\mathrm{API}_i = P_i - R_i + k_i \mathrm{API}_{i-1} \quad (5)$$

where R_i is the runoff but is not considered in this study because the API values have never exceeded the root zone saturation, API_{i-1} is the API value for day $i-1$, P_i is the accumulated precipitation (in mm) during day i, and k_i is the recession (or depletion) coefficient for day i. The coefficient k_i varies with time as a sinusoidal function with a period of 1 year, ranging from 0.92 to 0.94 from May to September (Choudhury and Blanchard, 1983). As seen in Equation (5), when there is no precipitation ($P_i = 0$) for an extended time period, the depletion coefficient will cause API to decrease greatly from the initial value.

Fractional soil moisture content (in percent) is estimated as the ratio of API to API_{max}, where API_{max} is assumed to be a saturation value of 40 cm (Chang and Wetzel, 1991). The volumetric soil moisture shown here is the product of the fractional soil moisture content and the saturation volumetric soil moisture, which depends on soil types. The saturation volumetric soil moisture we used in this study is 0.4499, an average value for 11 soil types (Pielke, 2002). API is initialized on 1 May 2000 with the accumulated precipitation during the month of April 2000, and then run through September based on Equation (5).

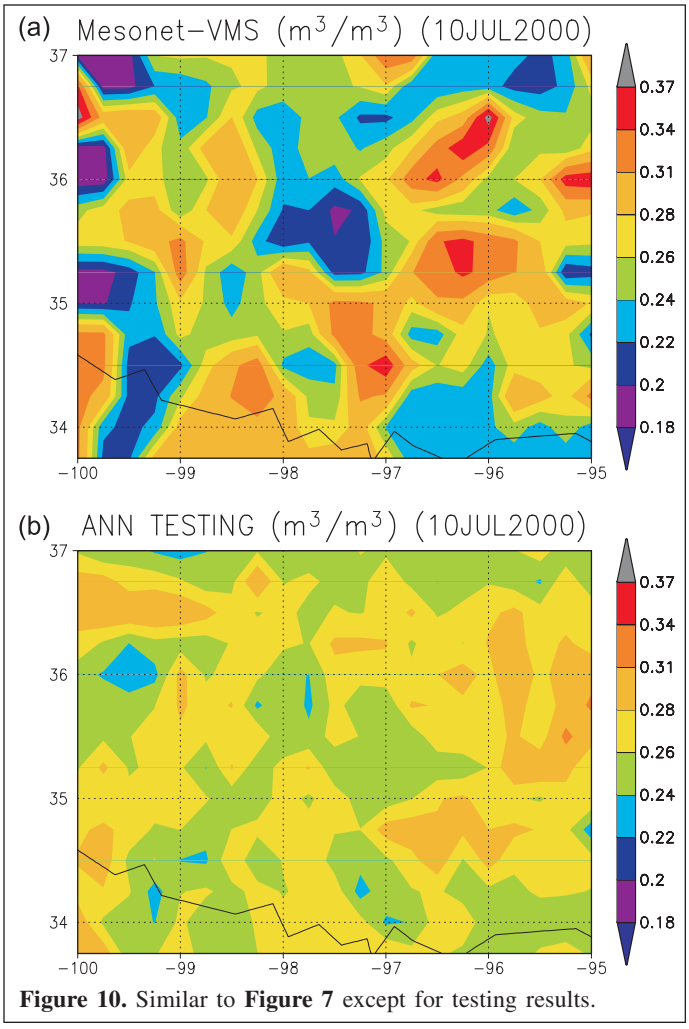

Figure 10. Similar to **Figure 7** except for testing results.

A plot similar to that of **Figure 8** is generated for the comparison between the Mesonet observation and the API estimate (**Figure 12**). The API (**Figure 12a**) systematically underestimates VSM for most of the time except for the month of June when surface precipitation was measured for most days (**Figure 12b**). As expected, the API estimate is strongly related to surface precipitation. The performance of the API model deteriorated with time (**Figure 12a**) as the effects of the initial API value became insignificant because of the depletion coefficient during the 2 month period between August and September when there is no measurable precipitation.

Summary

An artificial neural network (ANN) based methodology is introduced and tested for soil moisture estimation. We have shown that the ANN model can be trained to retrieve soil

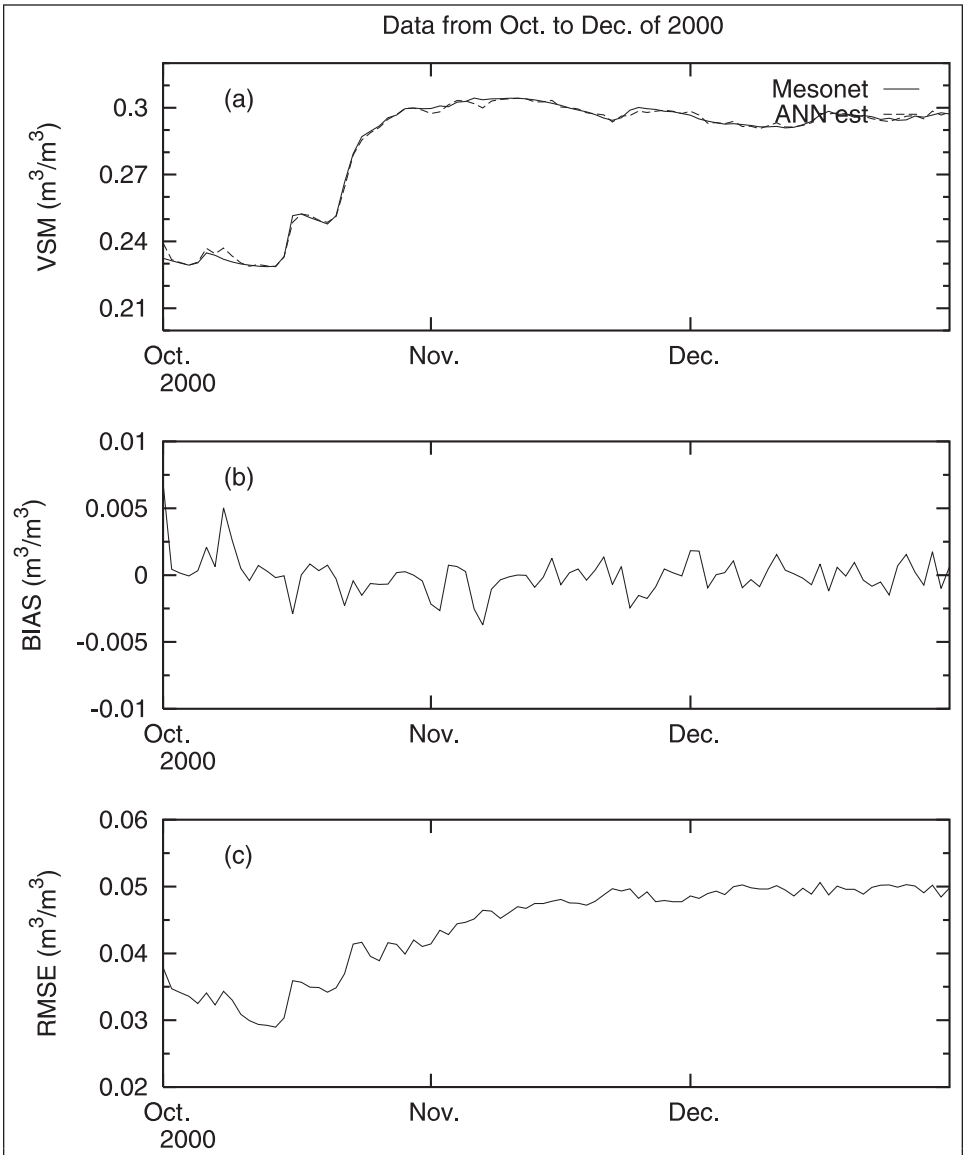

Figure 11. Similar to **Figure 8** except for comparison of statistical results from testing with data from the winter months of 2000 (Oct.–Dec.).

moisture information with the infrared (IR) skin temperature, previous 30 day accumulated surface precipitation, and vegetation index as the input variables. The ANN model has shown good performance when trained and tested with a spatially distributed dataset from a different season. The correlation coefficient for the relationship between the model estimate and the Mesonet-observed soil moisture is 0.9529 (**Figure 6**) for training and 0.9978 (**Figure 9**) for testing. The trained ANN model performed well when applied to an independent dataset from a different season. Comparison of the ANN estimation and the API reveals that the ANN model produces a more accurate estimation of soil moisture.

The biggest challenge to implementing the ANN model for real-time usage is to retrieve all the input variables directly from remotely sensed data with high spatial and temporal resolution. The ANN model has the following advantages over many other land-surface models: (*i*) soil moisture retrieval is not restricted to any model domain and can be extended to the entire globe; (*ii*) resolution can be as high as that of the input data (i.e., satellite-derived skin temperature, precipitation); and (*iii*) soil moisture can be retrieved for historical periods as long as the input data records are available.

Table 1. Correlation coefficients for the relationships between input variables T_s, N*, and PP and volumetric soil moisture (VSM).

Corr(input, VSM)	May–Sept.	Oct.–Dec.
Corr(T_s, VSM)	–0.4542	–0.5387
Corr(N*, VSM)	–0.5996	–0.1475
Corr(PP, VSM)	0.8851	0.5792

It should be mentioned that this ANN model has not been trained for the influence of antecedent snowpack. In

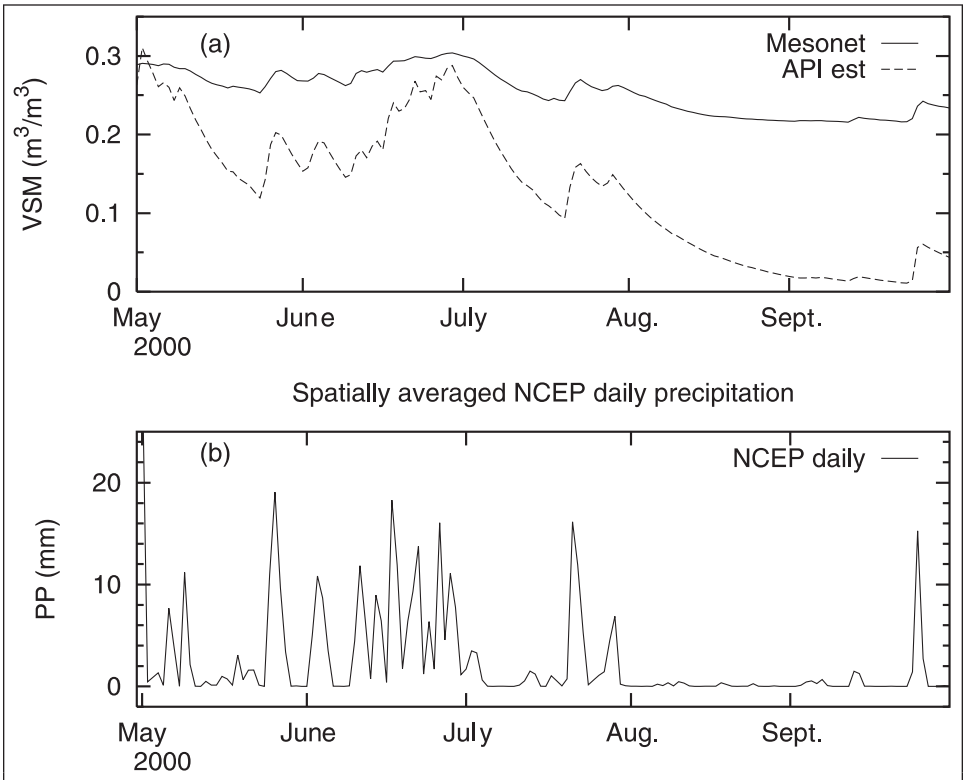

Figure 12. Comparison of soil moisture between API estimates and Mesonet measurements for the warm months of 2000 (May–Sept.).

mountainous regions and higher latitudes, snowmelt can be a dominant contributor to summertime soil wetness. Therefore a limitation of the current ANN model is that it has not been trained for those conditions.

This work has explored the applicability and potential of the ANN model in soil moisture estimation. The results from the ANN model are very encouraging for the cases tested. As satellite data become more and more available with improved spatial and temporal resolution, future work is needed in processing data directly acquired from remote sensing and training and validating the ANN model for use in regional or mesoscale modeling for soil moisture initialization.

Acknowledgments

The authors wish to thank Dr. Kuo-lin Hsu of the University of Arizona for providing the ANN model and answering questions related to the ANN model. We also thank Dr. Brian Cosgrove of the National Aeronautics and Space Administration (NASA) land data assimilation system (LDAS) group for his assistance in obtaining the skin temperature and NLDAS data. The comments of the anonymous reviewers greatly improved the clarity of this manuscript. This research was supported by a grant from NOAA under grant NA67-RJ0152 and by the National Science Foundation under grant ATM-0215367. The NDVI data are available from the US Geological Survey, EROS Data Center, Sioux Falls, South Dakota. The Mesonet data used in this study were obtained from the Joint Office for Science Support (JOSS) University Corporation for Atmospheric Research (UCAR) archive center.

References

Barnes, S.L. 1973. *Mesoscale objective analysis using weighted time-series observations*. National Severe Storms Laboratory, Norman, Okla. NOAA Technique Memo ERL NSSL-62 (NTISCOM-73-10781). 60 pp.

Blanchard, B.J., McFarland, M.J., Schmugge, T.J., and Thoades, E. 1981. Estimation of soil moisture with API algorithm and microwave emission. *Water Resources Bulletin*, Vol. 17, pp. 767–774.

Chang, J.-T., and Wetzel, P.J. 1991. Effects of spatial variations of soil moisture and vegetation on the evolution of a prestorm environment: a numerical case study. *Monthly Weather Review*, Vol. 119, pp. 1368–1390.

Choudhury, B., and Blanchard, B.J. 1983. Simulating soil water recession coefficients for agricultural watersheds. *Water Resources Bulletin*, Vol. 19, pp. 241–247.

Clark, C.A., and Arritt, R.W. 1995. Numerical simulations of the effect of soil moisture and vegetation cover on the development of deep convection. *Journal of Applied Meteorology*, Vol. 34, pp. 2029–2045.

Daamen, C.C., and Simmonds, L.P. 1996. Measurement of evaporation from bare soil and its estimation using surface resistance. *Water Resources Research*, Vol. 32, pp. 1393–1402.

Fast, J.D., and McCorkle, M.D. 1991. The effects of heterogeneous soil moisture on a summer baroclinic circulation in the central United States. *Monthly Weather Review*, Vol. 119, pp. 2140–2167.

Gallus, W.A., Jr., and Segal, M. 2000. Sensitivity of forecast rainfall in a Texas convective system to soil moisture and convective parameterization. *Weather Forecasting*, Vol. 14, pp. 509–525.

Gillies, R.R., and Carlson, T.N. 1995. Thermal remote sensing of surface soil water content with partial vegetation cover for incorporation into climate models. *Journal of Applied Meteorology*, Vol. 34, pp. 745–756.

Golaz, J.-C., Jiang, H., and Cotton, W.R. 2001. A large-eddy simulation study of cumulus clouds over land and sensitivity to soil moisture. *Atmospheric Research*, Vols. 59–60, pp. 373–392.

Hecht-Nielsen, R. 1988. Applications of counterpropagation networks. *Neural Networks*, Vol. 1, pp. 131–139.

Hsu, K.L., Gupta, H.V., and Sorooshian, S. 1995. Artificial neural network modeling of the rainfall–runoff process. *Water Resources Research*, Vol. 31, pp. 2517–2530.

Hsu, K.L., Gao, X., Sorooshian, S., and Gupta, H.V. 1997. Precipitation estimation from remotely sensed information using artificial neural networks. *Journal of Applied Meteorology*, Vol. 36, pp. 1176–1190.

Hsu, K.L., Gupta, H.V., Gao, X., and Sorooshian, S. 1999. Estimation of physical variables from multichannel remotely sensed imagery using a neural network: application to rainfall estimation. *Water Resources Research*, Vol. 35, pp. 1605–1618.

Jones, A.S., Guch, I.G., and Vonder Haar, T.H. 1998a. Data assimilation of satellite-derived heating rates as proxy surface wetness data into a regional atmospheric mesoscale model. Part I: methodology. *Monthly Weather Review*, Vol. 126, pp. 634–645.

Jones, A.S., Guch, I.G., and Vonder Haar, T.H. 1998b. Data assimilation of satellite-derived heating rates as proxy surface wetness data into a regional atmospheric mesoscale model. Part II: a case study. *Monthly Weather Review*, Vol. 126, pp. 646–667.

Kohonen, T. 1984. *Self-organization and associative memory.* Springer-Verlag, Berlin.

Mitchell, K.E., Lohmann, D., Houser, P.R., et al. 2004. The multi-institution North American Land Data Assimilation System (NLDAS): utilizing multiple GCIP products and partners in a continental distributed hydrological modeling system. *Journal of Geophysical Research*, Vol. 109, No. D7, D07S90, 10.1029/2003JD003823.

McNider, R.T., Song, A.J., Casey, D.M., Wetzel, P.J., and Crosson, W.L. 1994. Toward a dynamic–thermodynamic assimilation of satellite surface temperature. *Monthly Weather Review*, Vol. 122, pp. 2784–2803.

Owe, M., Van de Griend, A.A., De Jeu, R., De Vries, J.J., Seyhan, E., and Engman, E.T. 1999. Estimating soil moisture from satellite microwave observations: past and ongoing projects and relevance to GCIP. *Journal of Geophysical Research*, Vol. 104, pp. 19 735 – 19 742.

Pielke, R.A., Sr. 2002. *Mesoscale meteorological modeling*. Academic Press, New York.

Price, J.C. 1984. Land surface temperature measurements from the split window channels of the NOAA 7 advanced very high resolution radiometer. *Journal of Geophysical Research*, Vol. 89, pp. 7231–7237.

Rumelhart, D.E., Hinton, G.E., and Williams, R.J. 1986. Learning internal representation by error propagation. In *Parallel distributed processing: explorations in the microstructures of cognitions*. Edited by D.E. Rumelhart and J.L. McLelland. Massachusetts Institute of Technology Press, Cambridge, Mass. Vol. 1, pp. 318–362.

Sorooshian, S., Hsu, K.-L., Gao, X., Gupta, H.V., Imam, B., and Braithwaite, D. 2000. Evaluation of PERSIANN system satellite-based estimates of tropical rainfall. *Bulletin of the American Meteorological Society*, Vol. 81, pp. 2035–2046.

Teng, W.L., Wang, J.R., and Doraiswamy, P.C. 1993. Relationship between satellite microwave radiometric data, antecedent precipitation index, and regional soil moisture. *International Journal of Remote Sensing*, Vol. 14, pp. 2483–2500.

Tucker, C.J. 1979. Red and photographic infrared linear combinations for monitoring vegetation. *Remote Sensing of Environment*, Vol. 8, pp. 127–150.

Vinnikov, K.Y., Robock, A., Qiu, S., Entin, J.K., Owe, M., Choudhury, B.J., Hollinger, S.E., and Njoku, E.G. 1999. Satellite remote sensing of soil moisture in Illinois, United States. *Journal of Geophysical Research*, Vol. 104, pp. 4145–4168.

Wetzel, P.J., and Woodward, R.H. 1987. Soil moisture estimation using GOES-VISSR infrared data: a case study with a simple statistical method. *Journal of Climate and Applied Meteorology*, Vol. 26, pp. 107–117.

Wetzel, P.J., Atlas, D., and Woodward, R.H. 1984. Determining soil moisture from geosynchronous satellite infrared data: a feasibility study. *Journal of Climate and Applied Meteorology*, Vol. 23, pp. 375–391.